scientific reports

Check for updates

OPEN

Modeling of CO_2-LPG WAG with asphaltene deposition to predict coupled enhanced oil recovery and storage performance

Jinhyung Cho[1], Baehyun Min[2], Moon Sik Jeong[3], Young Woo Lee[3] & Kun Sang Lee[3]✉

Combined carbon capture and storage and CO_2-enhanced oil recovery (CCS-EOR) can reconcile the demands of business with the need to mitigate the effects of climate change. To improve the performance of CCS-EOR, liquefied petroleum gas (LPG) can be co-injected with CO_2, leading to a reduction in the minimum miscibility pressure. However, gas injection can cause asphaltene problems, which undermines EOR and CCS performances simultaneously. Here, we systematically examine the mechanisms of asphaltene deposition using compositional simulations during CO_2-LPG–comprehensive water–alternating-gas (WAG) injection. The LPG accelerates asphaltene deposition, reducing gas mobility, and increases the performance of residual trapping by 9.2% compared with CO_2 WAG. In contrast, solubility trapping performance declines by only 3.7% because of the greater reservoir pressure caused by the increased formation damage. Adding LPG enhances oil recovery by 11% and improves total CCS performance by 9.1% compared with CO_2 WAG. Based on reservoir simulations performed with different LPG concentrations and WAG ratios, we confirmed that the performance improvement of CCS-EOR associated with increasing LPG and water injection reaches a plateau. An economic evaluation based on the price of LPG should be carried out to ensure practical success.

Concerns about climate change are driving global efforts to reduce atmospheric CO_2 concentrations. Many options to reduce CO_2 emissions have been studied. Climate change mitigation will depend at least in part on combining CO_2 capture and utilization with microalgal carbon capture and biomass production[1]. Improving energy efficiency and using renewable energy in residential and industrial contexts can also reduce CO_2 emissions. Carbon capture and storage (CCS) is regarded as an effective way to reduce atmospheric CO_2 concentrations due to its negative CO_2 emissions[2,3]. Forty-three large-scale commercial CCS facilities were in operation globally in 2018[4], with that number increasing to 51 in 2019[5]. These operations have the combined capacity to capture and store an estimated 40 million tons of CO_2 every year. The disadvantage of CCS in aquifers is the lack of a profitability model. Coupling CO_2-enhanced oil recovery with CCS (CCS-EOR) could improve the economics through oil production[6,7].

Miscible gas flooding as an EOR technology changes the composition of oils and results in the precipitation and deposition of asphaltene in oil reservoirs[8] as changes in the composition of the oil affect the solubility of asphaltene[9,10]. Precipitated asphaltenes can be deposited throughout a reservoir, damaging geological formations. Such damage can affect both EOR performance and CO_2 storage mechanisms during CCS-EOR[11]. Oil and asphaltene do not have to be taken into account in conventional CCS involving aquifers. But in CCS-EOR, both the oil and asphaltene phases must be considered to enable precise performance predictions due to interactions among phases.

The effectiveness of CO_2 injection in CCS-EOR is limited due to difficulties reaching miscible conditions, which requires that the reservoir pressure exceed the minimum miscible pressure (MMP). Increasing only the injection pressure is challenging because of the cost and the risk of formation damage. Co-injection of liquefied petroleum gas (LPG) and CO_2 can address this problem by lowering the MMP instead of increasing reservoir

[1]Center for Climate/Environment Change Prediction Research, Ewha Womans University, 52 Ewhayeodae-gil, Seodaemun-gu, Seoul 03760, Republic of Korea. [2]Department of Climate and Energy Systems Engineering, Ewha Womans University, 52 Ewhayeodae-gil, Seodaemun-gu, Seoul 03760, Republic of Korea. [3]Department of Earth Resources and Environmental Engineering, Hanyang University, 222 Wangsimni-ro, Seongdong-gu, Seoul 04763, Republic of Korea. ✉email: kunslee@hanyang.ac.kr

pressure[12,13]. CO_2-LPG co-injection improves both the displacement and vertical-sweep efficiencies of EOR, but its effectiveness depends on other factors, such as heterogeneity and reservoir fluid properties[14,15]. Experimental studies of CO_2-LPG flooding have verified the advantages of LPG[12,13]. Because adding LPG accelerates oil swelling by improving miscibility and reducing oil density, it also intensifies asphaltene precipitation[16]. Previous studies assumed asphaltene only affected EOR, and not CO_2 storage[17,18]. To overcome these application limits, an integrative model that considers asphaltene deposition in a CO_2-LPG system was developed for this study. The model is an improved version of a CCS-EOR model developed by Cho et al.[11] that used only CO_2 injection. The new model can take into account the effects of both CO_2-LPG co-injection and formation damage on CO_2-trapping mechanisms during CCS-EOR.

Numerical model for major mechanisms. *Porosity and permeability reduction.* A solid model proposed by Gupta[19] was used for this study. Precipitating and non-precipitating components were used to calculate the fugacity of the solid phase[20]. While the solid model calculates the fugacity of the precipitating asphaltene, S_1, using Eq. (1), the Peng-Robinson equation of state (EOS)[21,22] computes the fugacity of the components in oil and gas phases:

$$\ln f_{S_1} = \ln f^*_{S_1} + \frac{V_{S_1}(p - p^*)}{RT} \tag{1}$$

where $f^*_{S_1}$ is the fugacity of S_1 at onset pressure p^* and V_{S_1} is the asphaltene molar volume. The equilibrium condition can be achieved when the fugacities of each component in solid (the solid model), water (Henry's law), oil, and gas (Peng-Robinson EOS) are equal. The amount of asphaltene precipitation can be estimated using the equilibrium condition.

After estimating asphaltene precipitation through the equilibrium condition of the fugacity of each component, the Wang and Civan[23] equation can be applied to estimate the amount of asphaltene deposition as follows:

$$\frac{V^{n+1}_{S_2^d} - V^n_{S_2^d}}{\Delta t} = \alpha C^{n+1}_{S_2^f} \phi^{n+1} - \beta V^{n+1}_{S_2^d} \left(v^n_o - v_{cr,o}\right) + \gamma u^n_o C^{n+1}_{S_2^f} \tag{2}$$

where $V_{S_2^d}$ and $C_{S_2^f}$ are the volume of deposited and flowing solid S_2 and v_o and $v_{cr,o}$ are the interstitial and critical velocity of the oil phase, respectively. The coefficient of the surface deposition is represented by α. The re-entrainment term β has a non-zero value when v_o is greater than $v_{cr,o}$ for the re-entrainment phenomenon, and can reduce the amount of asphaltene deposition. If v_o is lower than $v_{cr,o}$, β is set to zero and re-entrainment does not occur. The γ value is the pore throat-plugging coefficient.

Deposited asphaltene plug pores, which can reduce porosity and absolute permeability, are described by equations for the power law and the oil resistance factor[24]:

$$\phi = \phi_0 - V_{S_2^d} \tag{3}$$

$$\frac{k_0}{k} = \left(\frac{\phi_0}{\phi}\right)^n = F_{r,o} \tag{4}$$

where the superscript 0 refers to the initial condition and $F_{r,o}$ is the oil resistance factor.

Residual and solubility trapping. Asphaltene deposition not only changes absolute permeability but also relative permeability with wettability alterations[25]. To reflect this effect, the Brooks–Corey model is applied with the contact angle change[26]:

$$k_{r,w} = k^*_{r,w}\left(\frac{S_w - S_{r,w}}{1 - S_{r,w} - S_{r,nw}}\right)^{e_w} \tag{5}$$

$$k^*_{r,w} = 1 + \left[k^{0*}_{r,w} + \frac{\cos\theta - \cos\theta^0}{\cos\left(\pi - \theta^0\right) - \cos\theta^0}\left(k^{0*}_{r,nw} - k^{0*}_{r,w}\right) - 1\right]\left(\frac{1 + T^0_w N^0_{T,w}}{1 + T_w N_{T,w}}\right) \tag{6}$$

$$e_w = 1 + \left[e^0_w + \frac{\cos\theta - \cos\theta^0}{\cos\left(\pi - \theta^0\right) - \cos\theta^0}\left(e^0_{nw} - e^0_w\right) - 1\right]\left(\frac{1 + T^0_w N^0_{T,w}}{1 + T_w N_{T,w}}\right) \tag{7}$$

where subscript O indicates the initial condition, and w and nw indicate the wetting and non-wetting phases, respectively, k^*_r is the endpoint of the relative permeability, S_r is the residual saturation, e_w is the exponential parameter, and T_w and N_T are the trapping parameter and number, respectively.

Relative permeability and contact angle changes are assumed to be affected only by asphaltene deposition. The initial condition of reservoir is considered as strongly water-wet, changing to slightly water-wet at maximum asphaltene deposition, as determined by the interpolation method. To ensure reliability, the same reference is used for relative permeability and fluid data, which are widely used in asphaltene simulation studies, and a previous base study[11,27]. The reservoir gradually changes to slightly water-wet conditions using the interpolation method, depending on the amount of asphaltene deposition (Fig. 1).

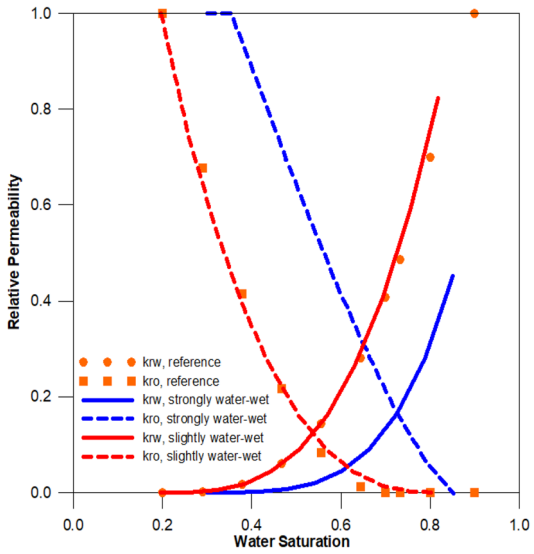

Figure 1. Water and oil relative permeability curves[11].

	Composition	p_c (kPa)	T_c (K)	Molecular weight	Acentric factor
CO_2	0.0246	7376.5	304	44.0	0.225
N_2	0.0057	3394.4	126	28.0	0.040
CH_4	0.3637	4600.2	191	16.0	0.008
C_2H_6	0.0347	4883.9	305	30.1	0.098
C_3H_8	0.0405	4245.5	369	44.1	0.152
IC_4	0.0059	3647.7	408	58.1	0.176
NC_4	0.0134	3799.7	425	58.1	0.193
IC_5	0.0074	3384.3	460	72.2	0.227
NC_5	0.0083	3374.1	469	72.2	0.251
FC_6	0.0162	3293.1	508	86.0	0.275
C_{7-15}	0.1966	2624.3	653	153.4	0.452
C_{16-25}	0.1255	1621.2	810	293.3	0.789
C_{26-30}	0.0400	1226.0	899	389.5	1.015
C_{31A+}	0.0742	689.01	1076	665.6	1.423
C_{31B+}	0.0433	689.01	1076	665.6	1.423

Table 1. Burke Oil 1 composition and properties.

The Larsen and Skauge[28] three-phase hysteresis model can be applied to reflect the residual trapping performance with the estimated relative permeability curves. Aziz and Settari[29] derived oil's relative permeability in a three-phase system from two-phase relative permeability data through a modified version of Stone's first model. Henry's law[30] estimates solubility-trapping performance. While an EOS calculates the fugacity of CO_2 in gas and oil phases, Henry's law calculates fugacity in the aqueous phase.

Results

Asphaltene and fluid modeling. In this study, fluid modeling for asphaltene precipitation and compositional simulations used WinProp and GEM, which were developed by the Computer Modelling Group Ltd. (CMG) in Canada[31,32].

Many simulation studies have used data from Burke Oil 1[33], which were also applied here[11,17]. Table 1 provides the oil composition and properties, and the experimental and calculated oil properties produced by a regression method are compared in Table 2, which shows the acceptable results. The MMP of Burke Oil 1, as estimated by the multiple-mixing-cell method, was 33,584 kPa with pure CO_2[34]. The MacLeod–Sugden correlation[35] was used to calculate the interfacial tension (IFT) between CO_2-LPG gas and crude oil. The MMP is considered when the IFT is less than 0.001 mN/m, and we used the same criterion in our study. Results of the MMP computation are shown in Table 3. The higher the LPG (63% propane and 37% butane) concentration, the lower the MMP, a trend that has been verified by previous studies[36,37].

Figure 2 depicts the amount of precipitated asphaltene versus CO_2 and LPG concentrations at a reservoir pressure of 15,857 kPa. The amount of precipitated asphaltene initially increased with the CO_2 mole fraction,

Parameter	Oil 1	Computed model
Saturation pressure (kPa)	20,339	20,340
Molecular weight (g/mol)	171	174
API (°)	19	19

Table 2. Oil properties of Burke Oil 1 data and the computed model.

Component	Multiple-mixing cell method	IFT method
CO_2	33,584	33,000
CO_2 90% + LPG 10%	30,681	29,000
CO_2 80% + LPG 20%	23,194	24,000

Table 3. MMP calculation results based on the multiple-mixing-cell and IFT methods (kPa).

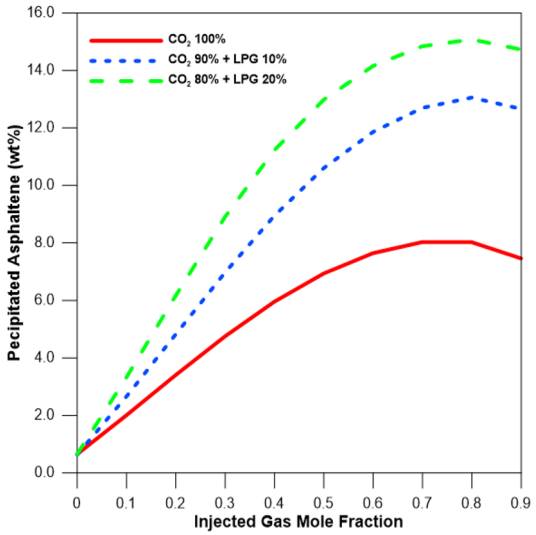

Figure 2. Amount of asphaltene precipitation with various CO_2 and LPG concentrations at a reservoir pressure of 15,857 kPa and a temperature of 100 °C.

but it began to decline after the injected gas mole fraction reached 0.7, likely because the saturation pressure also increased with CO_2 injection, making it a two-phase region[10]. The LPG accelerated more asphaltene precipitation relative to 100% CO_2 injection[16].

EOR performance. Because water–alternating-gas (WAG) injection increases the performance of both EOR and CCS, the process was applied in this study[38,39]. For the first three years, waterflooding was conducted as a secondary recovery, and WAG injection with a 1:1 ratio was performed for 10 years. All input parameters for the simulation are shown in Table 4.

Liquid propane gas can increase oil production by improving the displacement efficiency. The added LPG consists of 63% propane and 37% butane[30]. The enhanced displacement efficiency was confirmed by measurements of oil viscosity and density, and IFT changes. Figure 3 depicts the two-dimensional oil viscosity. In the blue region of the swept area where displacing fluids contact reservoir oil the most, the minimum oil viscosity obtained with 100% CO_2 injection is 1.02 mPa·s (Fig. 3a). When LPG was added as 10% of the molar fraction in the injected gas stream, the molecular weight and viscosity at the reservoir condition were 44.54 and 0.0673 mPa·s, respectively. The CO_2-LPG associated with the blue region spread more widely, and the oil viscosity decreased to 0.63 mPa·s, which was 38% lower than it in the CO_2 case (Fig. 3b). As the LPG concentration reached 20%, the oil viscosity decreased to 0.46 mPa·s (Fig. 3c). The white zone, which indicates a viscosity of greater than 5 mPa·s, spreads out near the injector because intermediate components were expelled from the initial oil, and heavier components accounted for a greater percentage of the residual oil. The zone becomes wider with increased LPG concentration due to the improved displacement efficiency. LPG also reduces oil mass density by accelerating oil swelling. Figure 4 illustrates the changes in oil density during WAG injection at the center of the reservoir. The minimum values were 841, 811, and 774 kg/m^3 for the 100% CO_2, 90% CO_2 + 10% LPG, and 80% CO_2 + 20% LPG cases,

Parameter	Value
Reservoir pressure (kPa)	27,580
Temperature (°C)	100
Permeability (m^2)	$1E^{-7}$
Porosity (%)	0.25
Initial oil saturation (S_o)	0.7
Bottom hole pressure (kPa)	19,300
Total gas injection (PV)	1
K_{12}	0.1
K_{21}	0.08
α	0.01
β	0
$v_{cr,o}$	0
γ	0.05
σ	150

Table 4. Simulation input data.

respectively, indicating that oil swelling was accelerated by the addition of LPG. In the area swept by the injected gas, oil density began to increase due to heavy components in the residual oil. Residual oil in the 80% CO_2 + 20% LPG WAG injection had the highest densities, which were 2% and 1% higher than in the 90% CO_2 + 10% LPG and 100% CO_2 cases, following the same trend as the residual oil viscosity.

The effect of LPG on the IFT change was investigated using IFT values plotted in the same area (Fig. 5). Because CO_2 and LPG co-injection increased the density of the displacing fluid (due to the higher molecular weight of LPG), the CO_2 and LPG mixture became similar to oil, resulting in IFT reduction. As a result, the IFT between the stream with 20% added LPG and the reservoir oil had the lowest value, 0.2 mN/m. The IFT values between the 100% CO_2 and 90% CO_2 + 10% LPG streams and the reservoir oil were 1.4 and 0.5 mN/m, which were 600% and 150% higher than that of the stream with 20% added LPG.

Although adding LPG can improve miscibility, it can also increase asphaltene-related deposition in the reservoir (Fig. 6). The first stage of asphaltene deposition resulted from pressure depletion during pre-waterflooding for three years (2007–2010), and the compositional change of oil caused deposition again after 2010 due to WAG injection. Figure 7 shows the effects of the oil resistance factor, with that of CO_2-LPG WAG injection 4% higher than it was in CO_2 WAG injection. Figure 8 supplies the water relative permeability curves after the wettability alteration by asphaltene deposition. Water permeability was enhanced to the water saturation (shown by the black line) after asphaltene deposition during CO_2 WAG injection. For CO_2-LPG WAG injection, the improvement was more significant, as indicated by the red line. Overall, LPG improved displacement efficiency, with oil 11% higher than in the case of CO_2 WAG injection (Fig. 9).

CCS-EOR performance. To exclude the effects of differences in the injection rates, the same rate was set for injected gas with molar fractions of 100% CO_2 and 90% CO_2 + 10% LPG. Figure 10 depicts the gas scanning curves for the asphaltene, hysteresis effects, and residual water saturation. Figure 10a shows the gas relative permeability change during CO_2 and CO_2-LPG WAG processes. Because LPG gives the rock surface a higher affinity for oil and gas due to surface deposition of asphaltene, the gas mobility decreased and the relative permeability shifted toward the bottom right. This caused 9% more CO_2 residual trapping by hysteresis, even though less injected CO_2 was involved in CO_2 WAG injection (Fig. 11). In contrast, because LPG accelerated the improvement of water mobility and gas hysteresis, trapped CO_2 displaced more water, reducing water saturation (Fig. 10b). Consequently, the CO_2 dissolved in the water in the CO_2-LPG WAG process was 3.9% lower than in the CO_2 WAG injection (Fig. 12). However, this does not indicate a reduced performance of CO_2 solubility trapping. Because the injected moles of CO_2 were different in this study, the ratio between the remaining and injected CO_2 in the reservoir should be compared when attempting to make an accurate comparison of trapping performance by mechanism (Fig. 13). The movable CO_2 was not yet trapped but can be trapped potentially. As shown in Fig. 13, residual trapped and movable CO_2 were 9.2% and 50% higher than in the CO_2 WAG case, respectively, while solubility-trapped CO_2 was 3.7% lower. The addition of LPG caused more wettability alteration, reduced gas mobility, and increased water mobility. Residual trapping performance was improved due to reduced gas mobility. In contrast, solubility trapping decreased because the increased water mobility reduced the residual water saturation. As a result, the total CCS performance was enhanced by 9.1% after the addition of LPG.

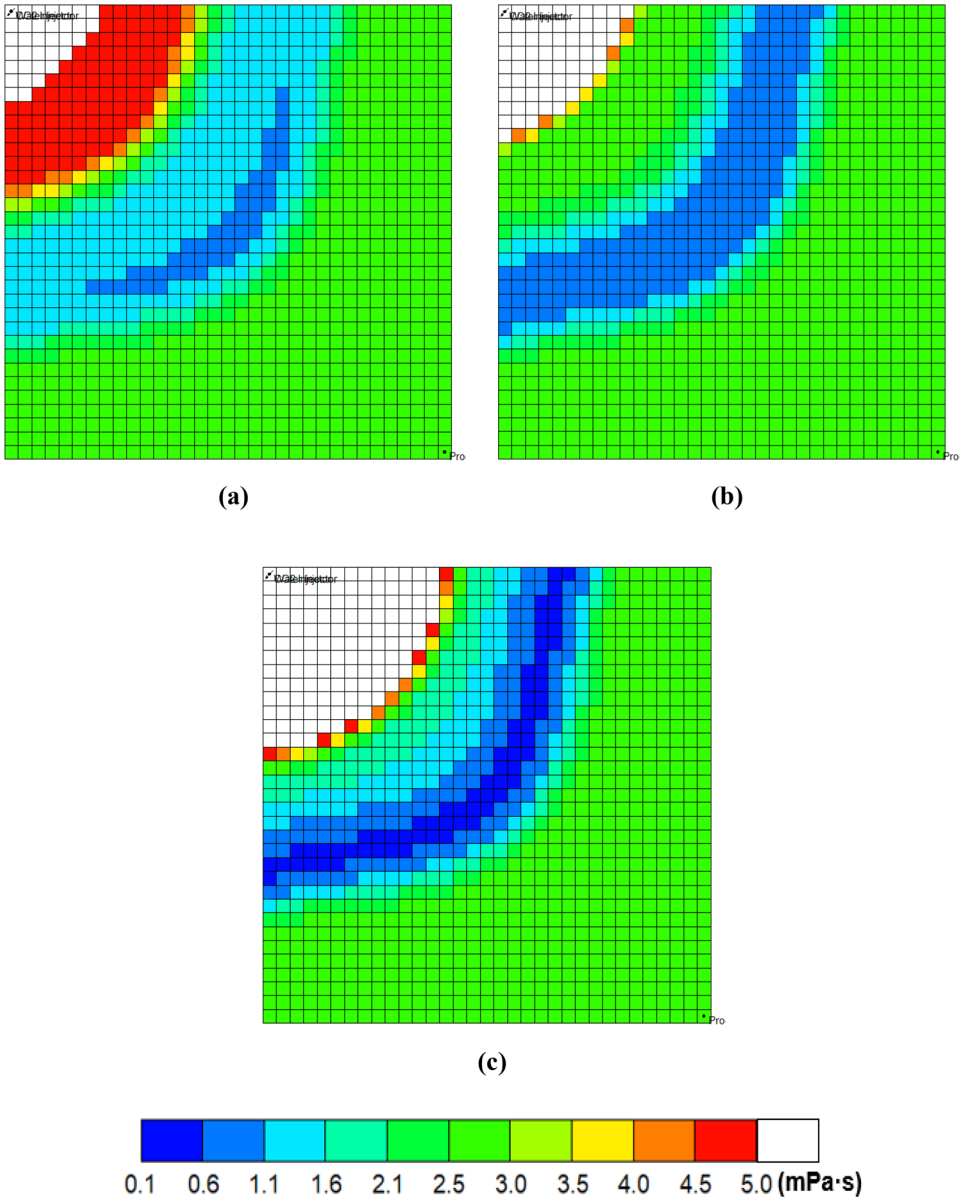

Figure 3. Oil viscosity with WAG: (**a**) 100% CO_2, (**b**) 90% CO_2 + 10% LPG, and (**c**) 80% CO_2 + 20% LPG after the first cycle of gas injection.

LPG concentration and WAG ratio effects. By analyzing the effectiveness of adding LPG to the CO_2 process, we investigated the effects of LPG concentrations and WAG ratios on CCS-EOR performance during CO_2-LPG WAG injection. As can be seen in Fig. 14, adding 10% LPG to the injection gas led to a 4% increase in oil recovery compared with 100% CO_2 injection. The recovery of 80% CO_2 + 20% LPG was 2% higher than that of the 90% CO_2 + 10% LPG case, and the increase was the same in the 30% LPG + 20% LPG conditions. This indicates that the incremental increase in EOR performance plateaus as the amount of added LPG increases.

The ratio between the remaining CO_2 in the reservoir and the injected CO_2 was compared for different LPG concentration models (Fig. 15). The performance of residual trapping was enhanced until the added LPG concentration reached 20% because the increased wettability reduced the gas mobility. When the added LPG concentration was increased to 30%, the efficiency of residual trapping did not change, as the wettability had already reached its maximum and the gas mobility was not further reduced. Because greater asphaltene deposition increased the reservoir pressure, solubility trapping was enhanced. In contrast, the average reservoir pressure increased due to more-severe plugging effects, and the solubility trapping performance could be enhanced. In summary, the ratios of residual to injected CO_2 were 50.7%, 55.3%, 61.3%, and 61.8% for cases with 100% CO_2 and 10%, 20%, and 30% LPG additions, respectively. The efficiency of CCS tended to be enhanced as the concentration of LPG increased. Economic analysis should be performed for both EOR and CCS, because the improved CCS efficiency with LPG addition shows diminishing returns.

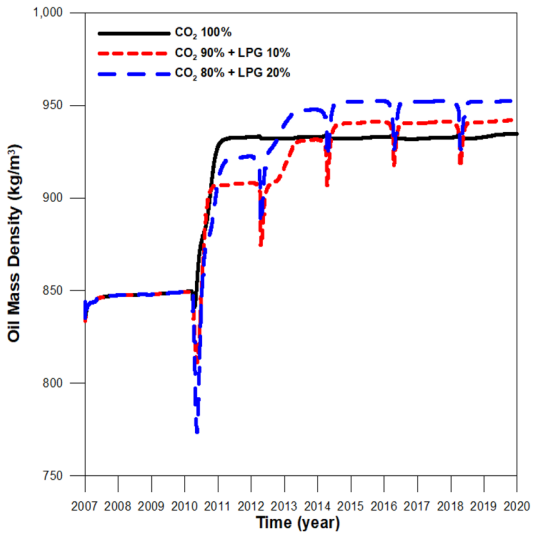

Figure 4. Oil density at the middle of the reservoir during CO_2 and CO_2-LPG WAG injection.

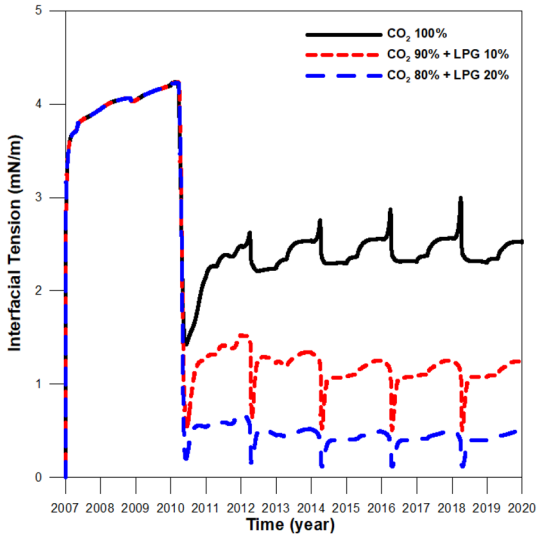

Figure 5. Interfacial tension values between injected CO_2-LPG gas and the reservoir oil during CO_2 and CO_2-LPG WAG injection.

To detect the effect of the WAG ratio, simulations were also conducted for models with WAG ratios of 1:1 (the previous model) and 2:1 (the amount of water injection was double compared to the previous model) during CO_2-LPG WAG. Because the same amount of gas was injected, the quantity of the deposited asphaltene was almost equal. However, the reservoir pressure increased due to greater water injection at a 2:1 WAG ratio (Fig. 16). The performance of CO_2 residual trapping in the 2:1 WAG model was less than that of the 1:1 model because the duration of each inhibition period was longer. This caused CO_2 to be expelled from trapped positions, despite the comparable amount of asphaltene deposition and wettability alteration. However, the higher reservoir pressure and greater water injection in the 2:1 WAG injection enhanced the performance of solubility trapping (Fig. 17). As a result, CCS performance did not change significantly, even though more water was injected in the 2:1 WAG injection. Increased water injection can therefore improve EOR performance with oil recovery by 1.1% (Fig. 18).

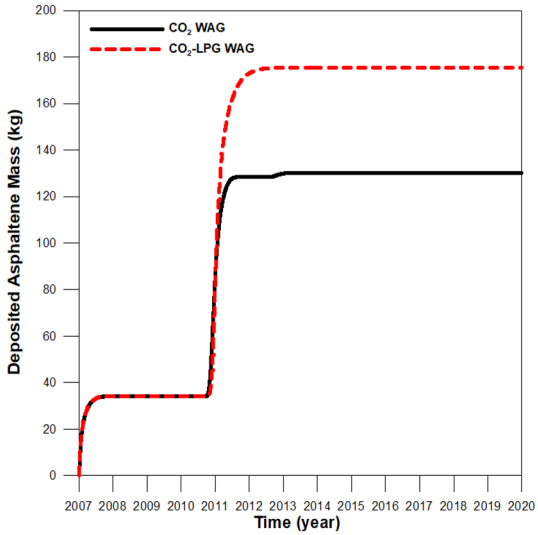

Figure 6. Asphaltene deposition at the middle of the reservoir during CO_2 and CO_2-LPG WAG injection.

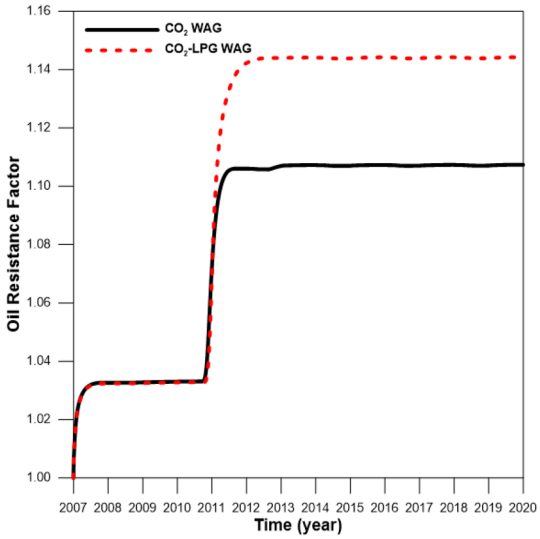

Figure 7. Oil resistance factor during CO_2 and CO_2-LPG WAG processes.

Discussion

This study examined the effects of adding LPG to an CO_2 stream in CCS-EOR with respect to asphaltene deposition using a compositional two-dimensional reservoir simulation. The effects of gravity and heterogeneity were ignored to focus on miscibility and damage to geological formations. We expect that the developed model can be expanded to a three-dimensional heterogeneous model that can be applied real field cases.

The significance and the speed of wettability alteration by asphaltene deposition remain controversial. Many studies, including this one, have assumed that wettability alteration depends on the amount of asphaltene deposition and the contact angle as determined by a computational method without experimental data[6,12,20,22]. This does not pose a logical problem, but it is necessary to select simulation parameters through experimentation to accurately evaluate the impact of asphaltene deposition on wettability alteration.

For field applications, an optimum CO_2-LPG WAG design that considers economic feasibility, such as tax credits; CAPEX; OPEX; and the price of CO_2, LPG, and oil, is necessary. Because these factors depend on reservoir characteristics, a site-specific design that incorporates economic feasibility is essential.

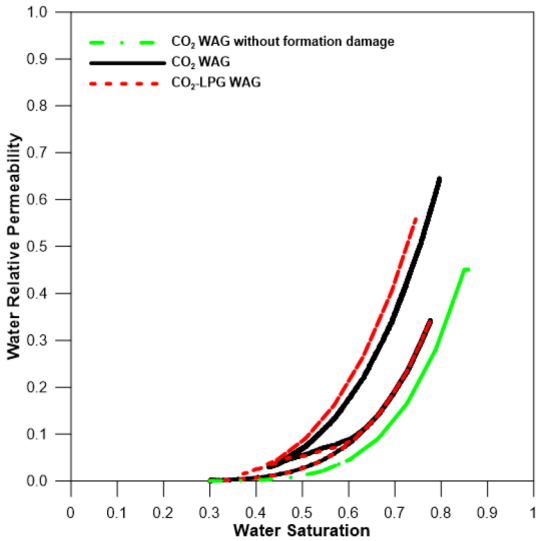

Figure 8. Water relative permeability with and without formation damage during CO_2 WAG and CO_2-LPG WAG injection.

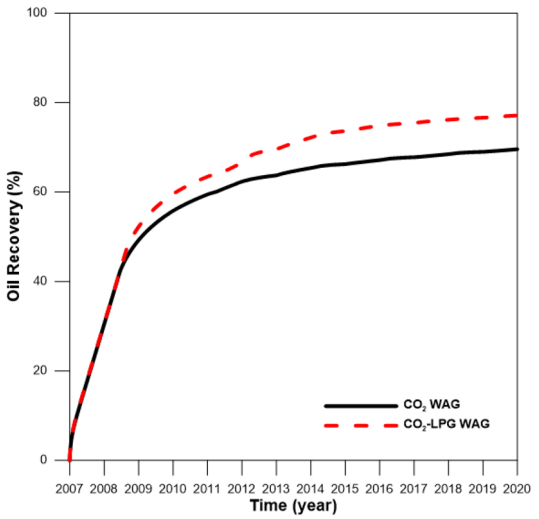

Figure 9. Oil recovery during CO_2 and CO_2-LPG WAG injection.

Conclusions

An integrated model that incorporates a fluid model with a reservoir simulation under dynamic conditions was developed to investigate the effects of LPG on a coupled CCS-EOR process with asphaltene deposition. For the reservoir simulation of WAG-based CCS-EOR, a three-phase hysteresis model was applied to determine trapping phenomena under dynamic conditions. Formation damage from asphaltene deposition was incorporated into models of the CO_2 and CO_2-LPG WAG processes. The following conclusions can be drawn:

1. Because of the improved displacement efficiency caused by the increased oil viscosity, increased density, and IFT reduction, LPG enhances EOR performance during WAG injection. Reduction in oil density by LPG addition lowers the asphaltene solubility of oil, and CO_2-LPG co-injection accelerates asphaltene precipitation and resulting formation damages. EOR performance of CO_2-LPG WAG injection without asphaltene 18% higher than that with asphaltene, according to the model. The performance of CO_2-LPG WAG injection can be overestimated if the formation damage is not considered.
2. An integrated model for CO_2-LPG WAG injection with three-phase hysteresis was applied to the coupled CCS-EOR process. LPG lowers oil density by more than does CO_2 WAG injection, and this accelerates asphaltene deposition. The residual trapping performance of CO_2-LPG WAG injection can be improved compared with CO_2 WAG injection. In contrast, more formation damages due to LPG addition lowers the solubility trapping performance compared with CO_2 WAG injection, although LPG increases the reservoir pressure.

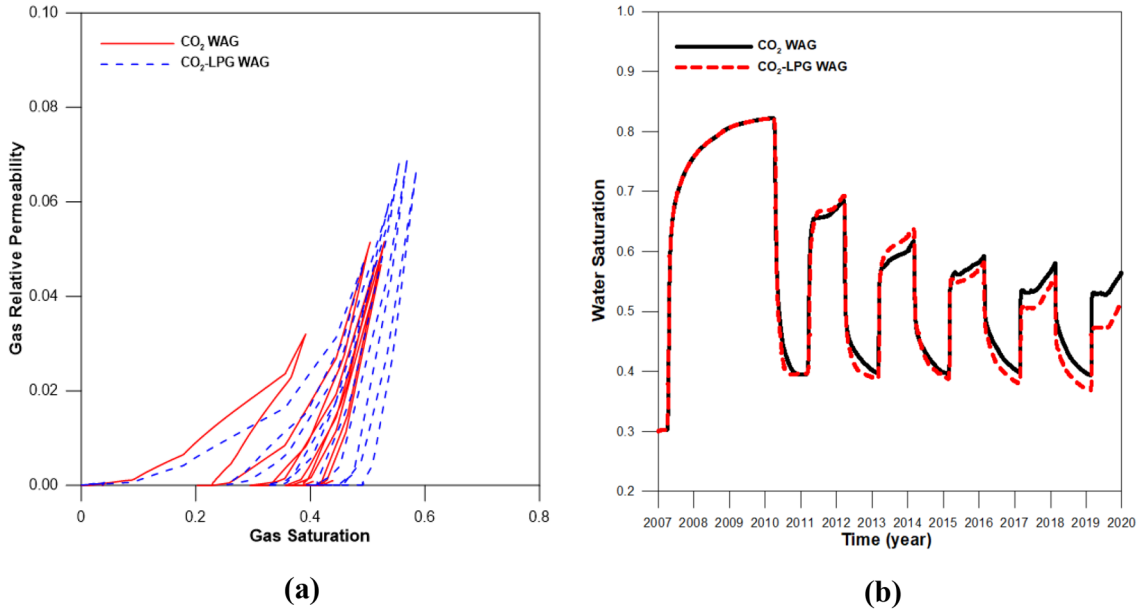

Figure 10. (**a**) Gas relative permeability and (**b**) residual water saturation during CO_2 and CO_2-LPG WAG injection.

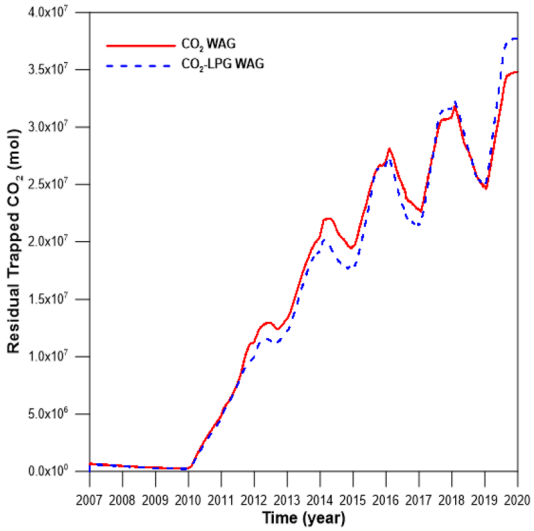

Figure 11. Residual trapped CO_2 for CO_2 and CO_2-LPG WAG models.

Adding LPG improves total CCS performance by 9.1% and enhances oil recovery by 11% compared with CO_2 WAG injection, and CO_2-LPG co-injection enhances not only EOR but also CCS performance during CCS-EOR.

3. To apply the integrative model in various conditions, reservoir simulations were conducted with different LPG concentrations and WAG ratios. Although both EOR and CCS performances can be enhanced at higher LPG concentrations, the increment becomes smaller with more LPG. Therefore, economic evaluations should consider the price of LPG to determine the optimum LPG concentration. WAG ratios of 1:1 and 2:1 can also be compared to investigate the effect of the injection scheme with the same amount of gas. Although the amount of injected water with a 2:1 WAG ratio is much greater, long-term CCS and EOR performances do not change meaningfully. However, short-term oil recovery can be enhanced by up to 9.4% due to higher pressures and sweep efficiency. For optimum application of CCS-EOR in terms of LPG concentration and WAG ratios, an economic analysis that considers the price of LPG and water should be undertaken.

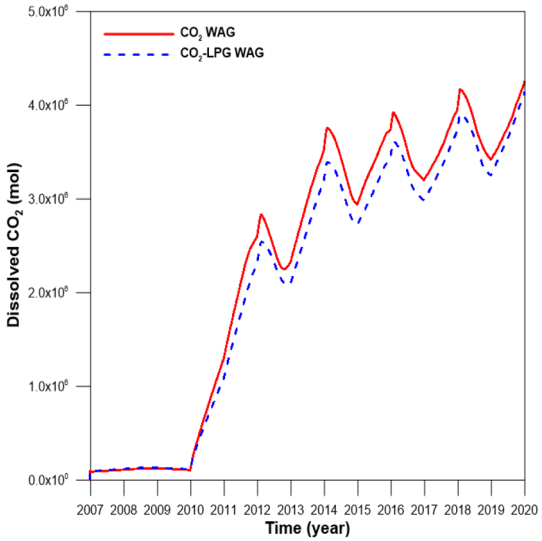

Figure 12. The amount of dissolved CO_2 for CO_2 and CO_2-LPG WAG injection.

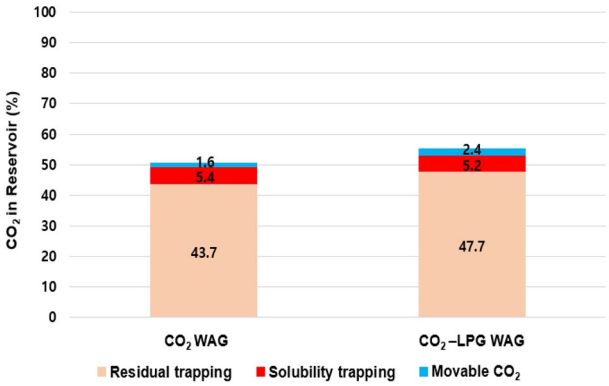

Figure 13. CO_2 remaining in the reservoir according to trapping mechanism.

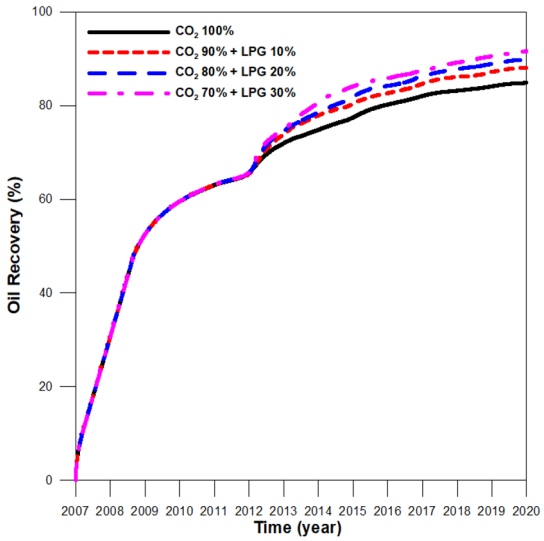

Figure 14. Oil recovery during CO_2 and CO_2-LPG WAG injection in integrative models at various LPG concentrations.

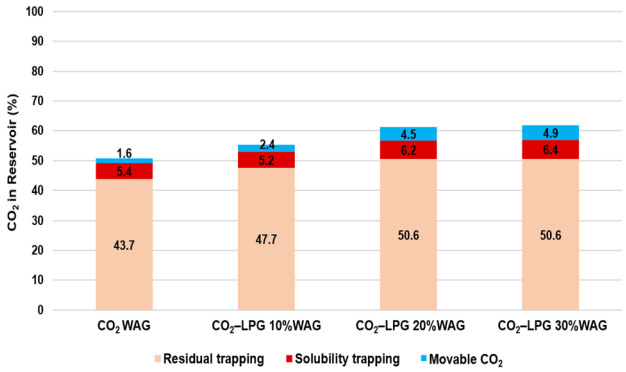

Figure 15. Remaining CO_2 in the reservoir according to trapping mechanism with various LPG concentrations.

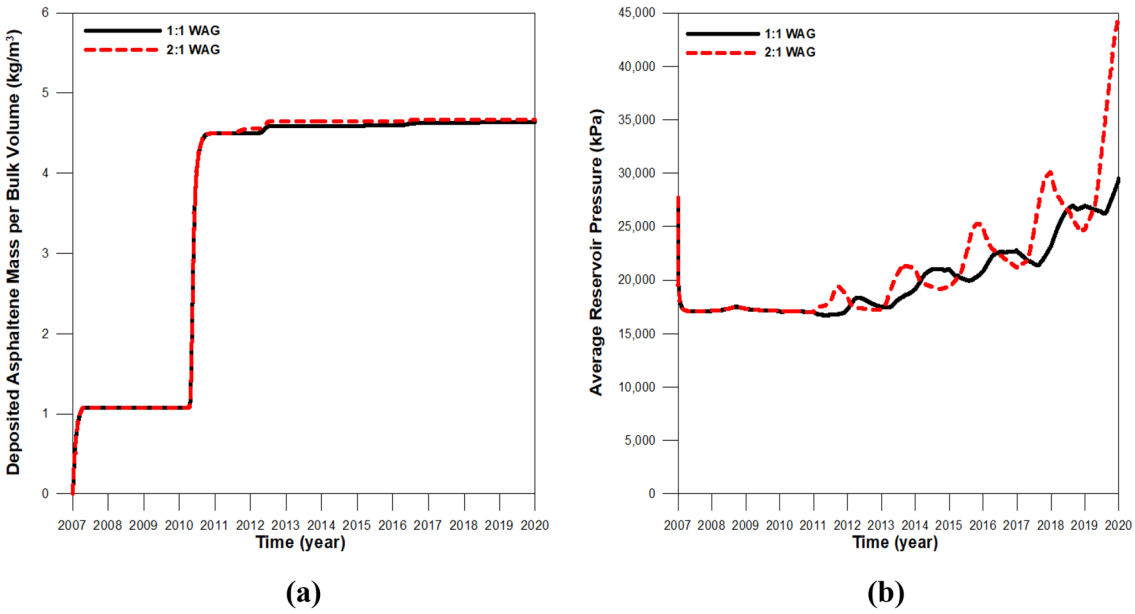

Figure 16. (**a**) The amount of asphaltene deposition per bulk volume in the middle of the reservoir and (**b**) the average reservoir pressure with different WAG ratios.

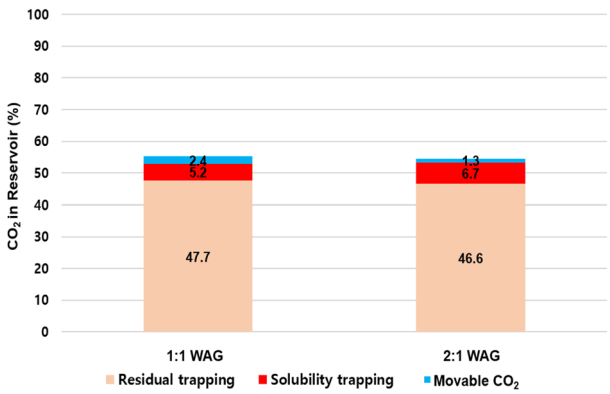

Figure 17. Remaining CO_2 in the reservoir according to trapping mechanism with various WAG ratios.

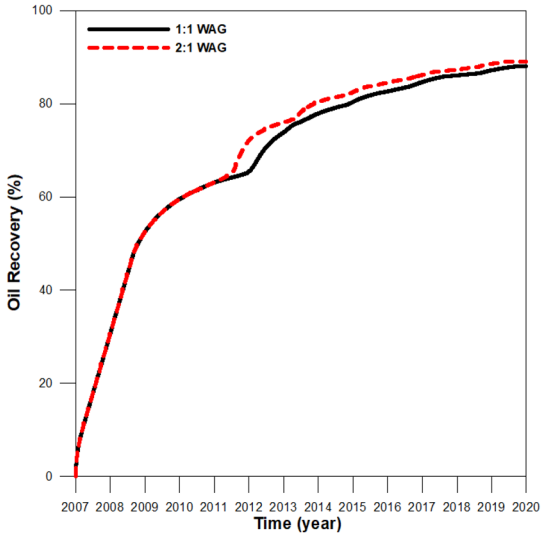

Figure 18. Oil recovery during CO_2-LPG WAG injection in integrative models with different WAG ratios.

Received: 14 July 2020; Accepted: 28 December 2020
Published online: 02 March 2021

References

1. Raslavicius, L., Striugas, N. & Felneris, M. New insights into algae factories of the future. *Renew. Sustain. Energy Rev.* **81**, 643–654 (2018).
2. IEA. *20 Years of Carbon Capture and Storage: Accelerating Future Deployment* (IEA Report, Paris, 2016).
3. Leung, D. Y. C., Caramanna, G. & Maroto-Valer, M. M. An overview of current status of carbon dioxide capture and storage technologies. *Renew. Sustain. Energy Rev.* **39**, 426–443 (2014).
4. Global CCS Institute. *The global status of CCS* (Global CCS Institute Report, Melbourne, 2018).
5. Global CCS Institute. *Global status of CCS* (Global CCS Institute Report, Melbourne, 2019).
6. IEA. *Storing CO_2 Through Enhanced Oil Recovery: Combining EOR with CO_2 Storage (EOR+) for Profit* (IEA Report, Paris, 2015).
7. IEA. *Transforming Industry Through CCUS* (IEA Report, Paris, 2019).
8. Tahami, S. A., Dabir, B., Asghari, K. & Shahvaranfard, A. Modeling of asphaltene deposition during miscible CO_2 flooding. *Pet. Sci. Technol.* **32**, 2183–2194 (2014).
9. Correra, S., Simoni, M.D., Bartosek, M., Colombani, G., Diatto, P., Maddinelli, G. & Parasiliti, V. Assessment of asphaltene deposition risk in an EOR intervention through CO_2 injection. *Paper presented at the SPE Annual Technical Conference and Exhibition, Florence, Italy, 19–22 September, 2010*.
10. Gonzalez, K., Barrufet, M.A. & Nasrabadi, H. Development of a compositional reservoir simulator including asphaltene precipitation from a thermodynamic consistent model. *Paper presented at the SPE Latin American and Caribbean Petroleum Engineering Conference, Maracaibo, Venezuela, 21–23 May, 2014*.
11. Cho, J., Kim, T. H., Chang, N. & Lee, K. S. Effects of asphaltene deposition-derived formation damage on three-phase hysteretic models for prediction of coupled CO_2 enhanced oil recovery and storage performance. *J. Petrol. Sci. Eng.* **172**, 988–997 (2019).
12. Shokir, E. M. E. M. CO_2–oil minimum miscibility pressure model for impure and pure CO_2 streams. *J. Petrol. Sci. Eng.* **58**, 173–185 (2007).
13. Talbi, K., Kaiser, T. & Maini, B. Experimental investigation of co-based vapex for recovery of heavy oils and bitumen. *J. Can. Pet. Technol.* **47**(4), 1–8 (2008).
14. Chugh, S., Baker, R., Cooper, L. & Spence, S. Simulation of horizontal wells to mitigate miscible solvent gravity override in the Virginia Hills Margin. *J. Can. Pet. Technol.* **39**(2), 28–34 (2000).
15. Cho, J. & Lee, K. S. Effects of hydrocarbon solvents on simultaneous improvement in displacement and sweep efficiencies during CO_2-enhanced oil recovery. *Pet. Sci. Technol.* **34**, 359–365 (2016).
16. Cho, J., Kim, T. H. & Lee, K. S. Compositional modeling of hybrid CO_2 EOR with intermediate hydrocarbon solvents to analyze the effect of toluene on asphaltene deposition. *J. Petrol. Sci. Eng.* **146**, 940–948 (2016).
17. Darabi, H., Sepehrnoori, K. & Kalaei, M.H. Modeling of wettability alteration due to asphaltene deposition in oil reservoirs. *Paper presented at the SPE Annual Technical Conference and Exhibition, San Antonio, Texas, USA, 8–10 October 2012*.
18. Wang, C., Li, T., Gao, H., Zhao, J. & Li, H. A. Effect of asphaltene precipitation on CO_2-flooding performance in low-permeability sandstones: A nuclear magnetic resonance study. *R. Soc. Chem.* **7**(61), 38367–38376 (2017).
19. Gupta, A.K. *A Model for Asphaltene Flocculation Using an Equation of State*. Master Thesis, University of Calgary (1986).
20. Kohse, B.F. & Nghiem, L.X. Modelling asphaltene precipitation and deposition in a compositional reservoir simulator. *Paper presented at the 2004 SPE/DOE Fourteenth Symposium on Improved Oil Recovery, Tulsa, Oklahoma, USA, 17–21 April, 2004*.
21. Peng, D. Y. & Robinson, D. B. A new two-constant equation of state. *Ind. Eng. Chem. Fundam.* **15**(1), 59–64 (1976).
22. Robinson, D.B. & Peng, D.Y. *The Characterization of the Heptanes and Heavier Fractions* (Gas Processors Association Report, 1978).
23. Wang, S. & Civan, F. Productivity decline of vertical and horizontal wells by asphaltene deposition in petroleum reservoirs. *Paper presented at the 2001 SPE International Symposium on Oilfield Chemistry, Houston, Texas, USA, 13–16 February, 2001*.
24. Reis, J. C. & Acock, A. M. Permeability reduction models for the precipitation of inorganic solids in Berea sandstone. *In Situ* **18**(3), 347–368 (1994).
25. Darabi, H., Shirdel, M., Kalaei, M.H. & Sepehrnoori, K. Aspects of modeling asphaltene deposition in a compositional coupled wellbore/reservoir simulator. *Paper presented at the SPE Improved Oil Recovery Symposium, Tulsa, Oklahoma, USA, 12–16 April, 2014*.

26. Lake, L. W., Johns, R. T., Rossen, W. R. & Pope, G. A. *Fundamentals of Enhanced Oil Recovery* (Society of Petroleum Engineers, Texas, 2014).
27. Fazelipour, W. Predicting asphaltene precipitation in oilfields via the technology of compositional reservoir simulation. *Paper presented at the SPE International Symposium on Oilfield Chemistry, Woodlands, Texas, USA, 11–13 April, 2011*.
28. Larsen, J. A. & Skauge, A. Methodology for numerical simulation with cycle-dependent relative permeabilities. *Soc. Petrol. Eng. J.* **3**(2), 163–173 (1998).
29. Aziz, K. & Settari, A. *Petroleum Reservoir Simulation* (Applied Science Publishers, London, 1979).
30. Li, Y. K. & Nghiem, L. X. Phase equilibria of oil, gas and water/brine mixtures from a cubic equation of state and Henry's law. *Can. J. Chem. Eng.* **64**(3), 486–496 (1986).
31. Computer Modeling Group. *GEM User Guide: Compositional & Unconventional Reservoir Simulator* (Computer Modeling Group User Manual, Calgary, 2019)
32. Computer Modeling Group. *WinProp User Guide: Phase Behavior & Fluid Property Program* (Computer Modeling Group User Manual, Calgary, Canada, 2019).
33. Burke, N. E., Hobbs, R. E. & Kashou, S. F. Measurement and modeling of asphaltene precipitation. *J. Petrol. Technol.* **42**(11), 1440–1446 (1990).
34. Ahmadi, K. & Johns, R. T. Multiple-mixing-cell method for MMP calculations. *Soc. Petrol. Eng. J.* **16**, 733–742 (2011).
35. Reid, R. C., Prautsnitz, J. M. & Sherwood, T. K. *The Properties of Gases and Liquids* 3rd edn. (McGraw-Hill, New York, 1977).
36. Metcalfe, R. S. Effects of impurities on minimum miscibility pressures and minimum enrichment levels for CO_2 and rich-gas displacements. *Soc. Petrol. Eng. J.* **22**, 219–225 (1982).
37. Teletzke, G.F., Patel, P.D. & Chen, A. Methodology for miscible gas injection EOR screening. *Paper presented at the SPE International Improved Oil Recovery Conference in Asia Pacific, Kuala Lumpur, Malaysia, 5–6 December, 2005*.
38. Sifuentes, W., Blunt, M.J. & Giddins, M.A. Modeling CO_2 storage in aquifers: assessing the key contributors to uncertainty. *Paper presented at the SPE Offshore Europe Oil & Gas Conference & exhibition, Aberdeen, UK, 8–11 September, 2009*.
39. Jun, W., Feng, W., Deping, Z., Guojun, Y., Ruosheng, P. & Shuai, X. CO_2 flooding WAG safety control technology. *Paper presented at the SPE Asia Pacific Oil and Gas Conference and Exhibition, Jakarta, Indonesia, 22–24 October, 2013*.

Acknowledgements

This work was supported by a National Research Foundation of Korea (NRF) grant funded by the Korean government (No. 2018R1A6A1A08025520 and No. 2020R1F1A1070406). Dr. Jinhyung Cho was supported by a NRF Grant (No. 2020R1I1A1A01067015).

Author contributions

J.C. designed the overall study and analyzed the results of this numerical work. J.C., B.M., M.S.J. and Y.W.L. reviewed and revised the manuscript. K.S.L. supervised the work.

Competing interests

The authors declare no competing interests.

Additional information

Correspondence and requests for materials should be addressed to K.S.L.

Reprints and permissions information is available at www.nature.com/reprints.

Publisher's note Springer Nature remains neutral with regard to jurisdictional claims in published maps and institutional affiliations.